

Heat Transfer Characteristics of a Quadratic Koch Island Fractal Heat Exchanger

JOSUA P. MEYER

Department of Mechanical and Aeronautical Engineering, University of Pretoria, South Africa

HILDE VAN DER VYVER

Department of Mechanical Engineering, Rand Afrikaans University, South Africa

Heat exchangers are widely used in the air conditioning and refrigeration industries, and any increase in their efficiency will have a positive effect on the industry as well. A new design of heat exchanger is proposed that will increase the heat transfer area significantly. The heat transfer area was increased by the use of fractals. Three techniques were used to investigate the heat transfer increase; analytical, numerical, and experimental methods. The results showed that the fractal heat exchanger has a higher heat transfer to overall volume ratio than a conventional tube-in-tube heat exchanger.

FRACTALS

The preparation of food, transport, and most work-related activities consume energy in the form of electricity, petrol, or natural gas. There are mainly two ways to save energy: by developing new energy sources and economizing on current energy use. In the United States, more than a third of the energy is used for water heating, space heating, air conditioning, and industrial petrochemical processes [1]. By designing innovations to reduce heat losses and increase thermal efficiencies, energy conversion processes can be made more economical [2]. Many energy conversion processes make use of heat exchangers.

To increase the heat transfer in an exchanger, several parameters could be changed, including the conduction and convection coefficients, the heat transfer area, and the temperature difference. An increase in any of those parameters would result in an increase in the heat flow. One method that could be used is to change the geometry of a heat exchanger to present a fractal profile (see Figure 1). The idea to use fractals to enhance the heat transfer came from an electrical application, where a fractal was used to increase the capacitance per unit area [3].

Benoit Mandelbrot coined the word *fractal* in the late 1970s for objects where the Hausdorff-dimension was not an integer

Address correspondence to Dr. Josua P. Meyer, Department of Mechanical and Aeronautical Engineering, University of Pretoria, Pretoria 0002, South Africa. E-mail: jmeyer@up.ac.za

but a fraction. In the normal understanding of the universe, a point has a dimension equal to zero, a line or curve has one dimension, points on a plane are two-dimensional, and any point in the universe that can be described by three coordinates is three-dimensional. The definition of a fractal was derived from the concept of dimensionality.

When an object is subdivided into N copies of itself and scaled down to scale f , the dimension D is defined as [4]

$$D = \frac{\log N}{\log \frac{1}{f}} \quad (1)$$

To calculate the dimension of the fractal that was used in this paper, the scale was taken as a quarter and the number of copies was multiplied by the sides of the square ($N = 4(8) = 32$). The Hausdorff dimension for the perimeter of the object in Figure 1 was calculated as:

$$D = \frac{\log 32}{\log 4} = 2.5 \quad (2)$$

There are various examples of fractal applications in thermodynamics and heat transfer. Fractals were used in the chemical combustion industry [5], and others [6] applied fractal theory to the optical properties of soot that affected the characteristics of flames.

Fractals were also applied to describe heat transfer parameters such as turbulent characteristics and conduction. The transition

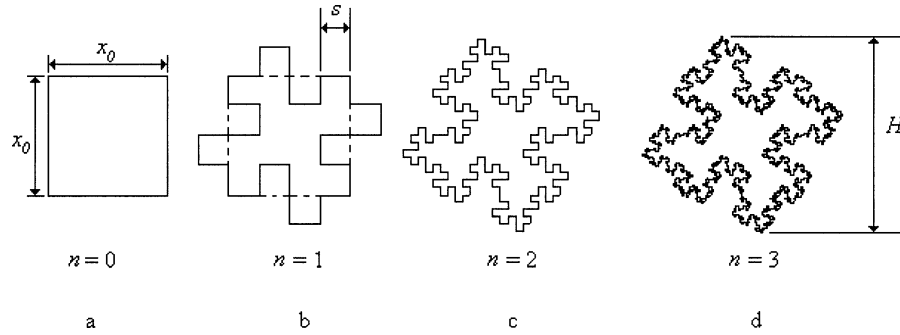


Figure 1 Quadratic Koch island fractal.

process from steady to turbulent convection was studied using numerical methods that showed a fractal structure [7].

Fractal and chaos analysis was applied to characterize the turbulence quality of the two mean velocity distributions of the circulating flow field [8]. Fractal theory was also used to study the conduction through a grooved surface [9]. A fractal model was introduced to predict the contact conductance resistance [10]. Fractals are applied in the heat conduction application by using the local fractal dimension to characterize the arrangement of fibres in a composite [11].

A heat transfer application was recently published by Chen and Cheng [12] that used a fractal tree-like microchannel net for electronic cooling.

FRactal Tube

For this study, the fractal was applied to the inner tube of a tube-in-tube heat exchanger. The area, length, circumference, and overall length of the fractal heat exchanger were dependent on the amount of times the fractal has been applied. Thus, the correlation between the area, circumference, and fractal iteration was derived for a quadratic Koch island fractal.

Cross-Sectional Area

The overall area of the block with side length of x_0 (refer to Figure 1a) did not change, because when a fractal area was added, the same area was subtracted elsewhere. Thus,

$$A_n = A_0 = x_0^2 \tag{3}$$

The cross-sectional area of a quadratic Koch island fractal, therefore, remained constant and was not a function of the number of times the fractal was applied.

Circumference

The circumference of the block doubled every time the fractal was applied, and was equal to

$$C_n = 4(2^n x_0) \tag{4}$$

As n increased, the circumference increased as well. The heat transfer area was the product of the circumference and length of the exchanger. Thus, the heat transfer area increased with every application of the fractal.

HEAT TRANSFER CHARACTERISTICS

An estimation was done on the fractal heat exchanger to find the approximate heat transfer increase. The thickness of the fractal tube was disregarded in this estimation. Figure 2 is a representation of the fractal heat exchangers after zero and one application of the fractal. The inner diameter, d , of the outer tube is also shown.

This fractal heat exchanger with $n = 1$ (see Figure 2b) was compared to the benchmark heat exchanger ($n = 0$), which was a square tube in round tube heat exchanger (see Figure 2a). The inner tube had an outside width of d_o and a width of d_i . The thickness of the inner tube was defined as

$$\Delta d = \frac{d_o - d_i}{2} \tag{5}$$

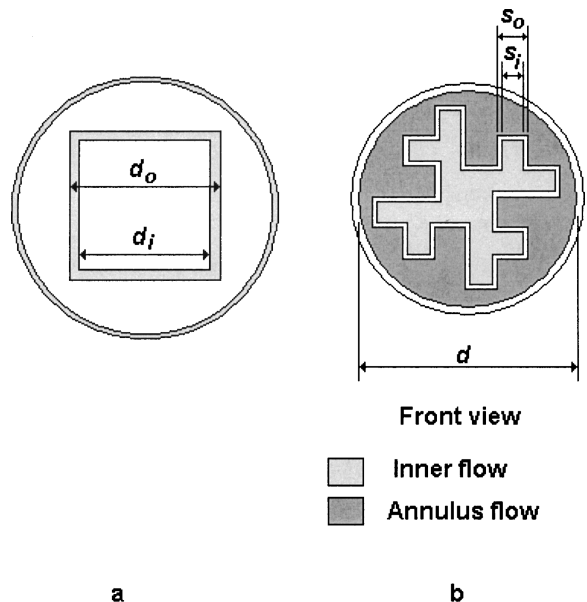


Figure 2 Front view of the fractal heat exchanger: a, $n = 0$; b, $n = 1$.

The hydraulic diameters were derived first, after which the Reynolds number equations were found. The hydraulic diameter for the inner tube was calculated as

$$d_{h,i} = \frac{4A_i}{p_{w,i}} = \frac{4d_i^2}{4 \cdot 2^n d_i} = \frac{d_i}{2^n} \quad (6)$$

Inserting Eq. (6) into the definition of the Reynolds number, the following was found for the inner tube:

$$\text{Re}_i = \frac{\rho v_i d_{h,i}}{\mu_i} = \frac{\rho v_i d_i}{2^n \mu_i} \quad (7)$$

The hydraulic diameter for the outer tube was calculated as

$$d_{h,o} = \frac{4A_o}{p_{w,o}} = \frac{4\left(\frac{1}{4}\pi d^2 - d_o^2\right)}{\pi d + 4 \cdot 2^n d_o} = \frac{\pi d^2 - 4d_o^2}{\pi d + 4 \cdot 2^n d_o} \quad (8)$$

The Reynolds number for the annulus was determined as:

$$\text{Re}_o = \frac{\rho v_o d_{h,o}}{\mu_o} = \frac{\rho v_o}{\mu_o} \left(\frac{\pi d^2 - 4d_o^2}{\pi d + 4 \cdot 2^n d_o} \right) \quad (9)$$

As noted before, for the estimation process, the thickness of the fractal tube will be neglected; however, for simulation and experimental purposes, the thickness has to be included. Comparing Figure 2 to Figure 1, it can be seen that the fractal length, s , was replaced by an inner (s_i) and outer (s_o) fractal length to compensate for the thickness. It follows that when dimensioning the fractal, the outer fractal length should be at least the sum of the inner fractal length and twice the thickness. Another consequence of having different fractal lengths is that the area calculation is not simply sixteen times the fractal length squared ($16s^2$); instead, each fractal cross-section should be carefully considered to determine the area. Having established the basic equations for the fractal heat exchanger, the heat transfer was then determined.

The heat transfer analysis is dependent on the type of heat flow. Examples of different flow arrangements are parallel flow, counterflow, and crossflow. For this paper, the setup was counterflow, with hot water flowing in the inner tube and the cold water in the annulus in the opposite direction.

The first law of thermodynamics was applied to the counterflow system to estimate the change in heat transfer. The first law was simplified by assuming that the flow was steady-state and the system was overall adiabatic. The heat transfer was expressed in terms of mean quantities [13]:

$$q = UA\Delta T_{LMTD} \quad (10)$$

U is the overall heat transfer coefficient, and is shown below:

$$U_i A_i = \frac{1}{\frac{1}{h_i A_i} + \frac{\Delta d}{4k2^n d_i L} + \frac{1}{h_o A_o}} \quad (11)$$

where

$$A_i = 4d_i 2^n L \quad (L \text{ is the length of the exchanger}) \quad (12)$$

$$A_o = 4d_o 2^n L \quad (13)$$

These equations assume a non-compact exchanger, so there is a limitation on the fractal iteration. For non-compactness, the surface area density on any fluid side should be less than $400 \text{ m}^2/\text{m}^3$. For the dimensions chosen, $n \leq 5$ [14].

For the estimation process, it was assumed that h_o and h_i would remain unchanged and are unaffected by the fractal. After substituting Eqs. (12) and (13) into (11) and simplifying, the following was found:

$$U_i = \frac{1}{\frac{1}{h_i} + \frac{\Delta d}{k} + \frac{d_i}{h_o d_o}} \quad (14)$$

Thus, the heat transfer becomes

$$q_i \propto 2^n (q'_i) \quad (15)$$

where q'_i is the heat transfer without the fractal application. The above analysis did not take into account the dependence of the heat transfer coefficients (h) on the fractal iteration. It is estimated that the heat transfer coefficient increases with fractal iteration: the dimensionless number, the Nusselt number, contains h . The Ditus-Boelter correlation for inner flow is shown below [13]:

$$\text{Nu}_i = 0.023 \cdot \text{Re}_i^{0.8} \text{Pr}_i^{0.3} \quad (16)$$

Inserting the definition of the Reynolds number (Eq. [7]) into the above equation yields:

$$\text{Nu}_i = 0.023 \cdot \left(\frac{\rho v_i d_i}{2^n \mu} \right)^{0.8} \text{Pr}^{0.3} \quad (17)$$

Therefore, the Nusselt number decreases with the fractal iteration:

$$\text{Nu}_i \propto 2^{-0.8n} \quad (18)$$

To establish the relation between the heat transfer coefficient and the fractal iteration, the definition of the Nusselt number is shown below:

$$\text{Nu}_i = \frac{h_i d_i}{2^n k} \propto 2^{-n} h_i(n) \quad (19)$$

Equating Eq. (18) and (19) results in:

$$h_i \propto 2^{0.2n} \quad (20)$$

The heat transfer coefficient increases with an increase in the fractal iteration. This estimation also holds for the annulus flow. Thus, the expected increase in heat transfer would be larger than Eq. (15) shows.

From Eq. (15), it followed that an increase of 100% could be expected for a fractal heat exchanger with each iteration. Unfortunately an increase in heat transfer is usually counteracted by an increase in pressure drop. The CFD analysis considered the heat transfer and the required pumping power through the exchanger.

Table 1 Properties of the CFD fractal heat exchangers

Properties	$n = 0$	$n = 1$	$n = 2$
Amount of iterations at convergence	60 to 92	51 to 69	90 to 92
Inner tube inside width	42 mm	n/a	n/a
Inner tube thickness	1 mm	1 mm	n/a
Inner diameter of outer tube	90 mm	90 mm	90 mm
Length of heat exchanger	125 mm	250 mm	125 mm
Inner hydraulic diameter	42 mm	20.2 mm	10.5 mm
Annulus hydraulic diameter	38.6 mm	26.6 mm	19.3 mm
Total volume of exchanger	199 mm ²	398 mm ²	199 mm ²
Amount of inner (hot) fluid cells	157165	105660	179200
Amount of annulus (cold) fluid cells	146200	181200	322000
Amount of tube cells	43860	62640	35840
Inner velocity range (corresponding Reynolds number range)	0.08 to 0.8 m/s (9394 to 93944)	0.08 to 0.8 m/s (4527 to 45272)	0.32 to 1.5 m/s (9385 to 43995)
Annulus velocity range (corresponding Reynolds number range)	0.17 to 1.7 m/s (5004 to 50039)	0.17 to 1.7 m/s (3450 to 34504)	0.9 to 3 m/s (13235 to 44117)
Heat balance error	5.3%	4.4%	4.7%

COMPUTATIONAL FLUID DYNAMICS

Three different fractal heat exchangers, corresponding to $n = 0, 1,$ and $2,$ were modeled numerically with a commercial CFD code. The simulation package used is called Star-CD and makes use of the finite volume method. The boundary conditions, fluid properties, etc., for each of the fractal heat exchangers were the same and are summarized below. CFD utilizes the differential forms of the Navier-Stokes equations to model fluid flow, and the κ - ϵ model for standard turbulent flow was used for the simulations. Heat transfer was modeled through the enthalpy conservation equation.

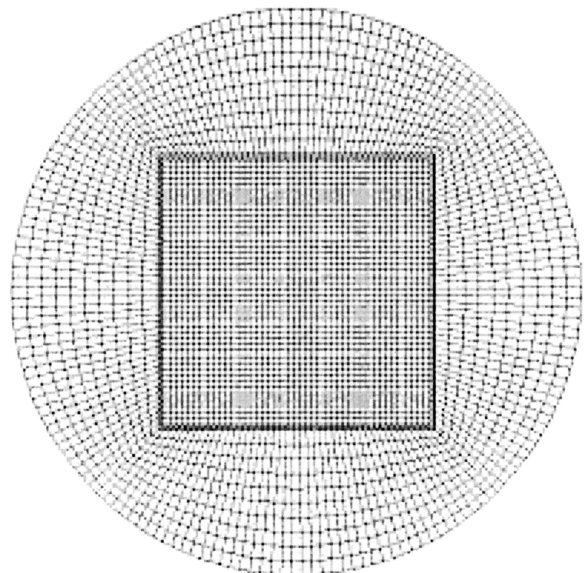
The turbulence intensity was 0.05, and the entrance length was 0.0005 m. Thus, the flow is not fully developed at the inlet but becomes fully developed very early in the flow. The same condition applies to the annulus flow, with the same turbulence intensity and a slightly higher entrance length of 0.0024 m. The increase in entrance length was done to keep the ratio of the entrance length to cross-section area the same for the inner and annulus flow.

The tube was modeled with aluminium because aluminium would be used in the experimental part of the study. The aluminium tube had a density of 2787 kg/m³, a conductivity of 164 W/mK, and a specific heat of 883 J/kgK. The inner inlet temperature was taken as 82°C (355 K) with a density of 970.2 kg/m³ and a viscosity of 3.47×10^{-4} kg/ms. For the annulus flow, the inlet temperature was 10°C (283 K) with a density of 999.2 kg/m³ and a viscosity of 1.31×10^{-3} kg/ms. The outer tube is not modeled: its presence is accounted for by introducing an adiabatic boundary at the top of the outer fluid.

For the second iteration, the aluminium tube was not modeled because of the limit of the amount of cells that the commercial code was able to handle. It was modeled with two-dimensional baffle cells. The properties of the aluminium tube were given in terms of the resistance, which is the thickness of the tube divided by the area of the tube, and conductivity, which is a very

small value. The baffle was defined as a conduction baffle so that heat transfer across the baffle could take place. For each inner Reynolds number, four simulations were done for the four annulus Reynolds numbers; thus, there were sixteen simulations in total. The physical properties of the three configurations are summarized in Table 1.

Cross-sections of the CFD grid of the exchangers are shown in Figures 3 to 5. For the exchanger with $n = 1$ and $n = 2,$ sixteen different tests were done on each of the CFD models. Table 1 shows the velocity ranges of the simulations as well as the heat balances. Figure 6 shows the heat transfer per unit length as a function of the inner and annulus velocities. The models were compared on a velocity bases, as the Reynolds number changes with the application of the fractal iteration when all other parameters (including velocity) remain constant.

**Figure 3** The fractal heat exchanger, $n = 0.$

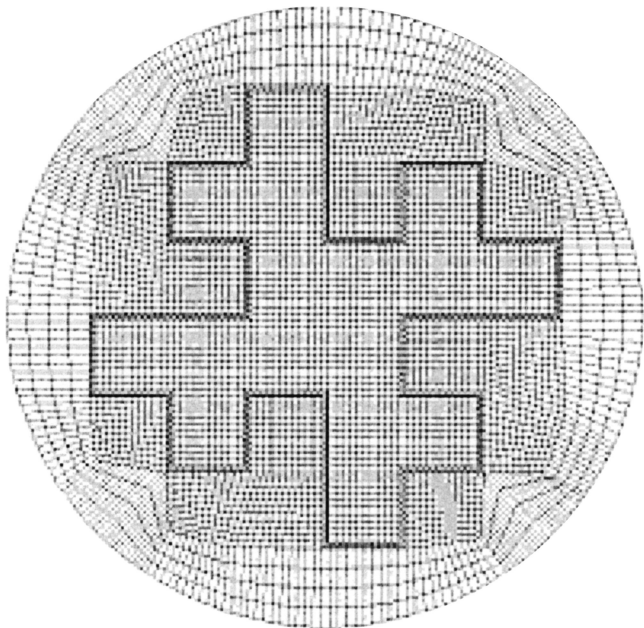


Figure 4 The fractal heat exchanger, $n = 1$.

From the above figures, it can be seen that the heat transfer increased with every application of the fractal iteration:

$$\frac{\left(\frac{q}{L\sqrt{v_i \cdot v_o}}\right)_{n=1}}{\left(\frac{q}{L\sqrt{v_i \cdot v_o}}\right)_{n=0}} \quad (21)$$

The average increases were, respectively, 2.1 and 3.5 times. If the very low values were disregarded (at low annulus Reynolds number), then the average increases were 3.9 for $n = 2$. The trend of heat transfer was what was expected from the analytical study, namely, 2^n . As the heat transfer increases, more effort is

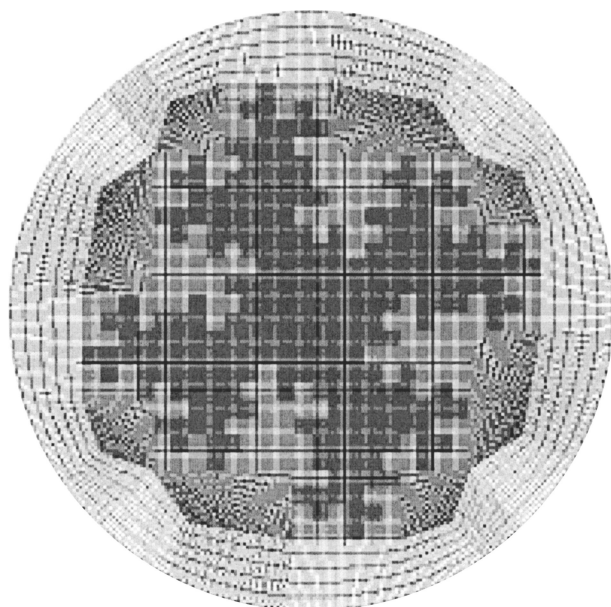


Figure 5 The fractal heat exchanger, $n = 2$.

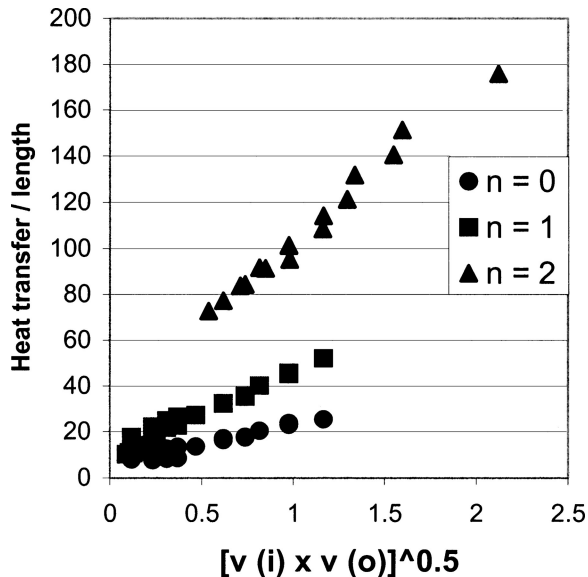


Figure 6 CFD heat transfer of the fractal heat exchangers as a function of the velocities.

needed to pump the fluid through the exchanger. Figure 7 shows the relation of heat transfer per total pumping power (inner plus annulus) for the three exchangers. From the figure, it can be seen that for $n = 0$ and 1, there is little difference between the ratios of the heat transfer to pumping power. However, for $n = 2$, the ratio decreases as the pumping power increases at a higher rate than the heat transfer.

The increase in pumping power is given as

$$\frac{\left(\frac{P_i + P_o}{L\sqrt{v_i \cdot v_o}}\right)_{n=1}}{\left(\frac{P_i + P_o}{L\sqrt{v_i \cdot v_o}}\right)_{n=0}} \quad (22)$$

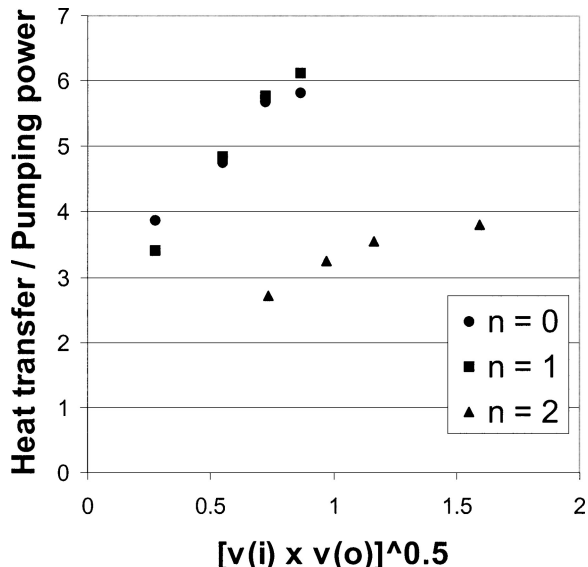


Figure 7 CFD heat transfer over total pumping power.

Table 2 Physical measurements of the fractal heat exchanger

Heat exchange length	3910 mm
Outside diameter of round tube	88.9 mm
Inside diameter of round tube	79.34 mm
Outer fractal length, s_o	13 mm
Inner fractal length, s_i	7 mm
Inner cross-sectional area	$1 \times (17)(17) + 4 \times (10)(7) + 4 \times (7)(20) = 1129 \times 10^{-6} \text{ m}^2$
Outer cross-sectional area	$1 \times (23)(23) + 12 \times (10)(13) = 2089 \text{ mm}^2$ (including thickness) $\frac{\pi d^2}{4} - 2089 \times 10^{-6} = 2855 \times 10^{-6} \text{ m}^2$
Overall volume	0.02427 m^3
Inner hydraulic diameter	14.662 mm
Outer hydraulic diameter	19.647 mm

Table 3 Heat exchanger of $n = 0$

Annulus cross-sectional area	0.003376 m^2
Inner circumference area	0.5255 m^2
Annulus circumference area	0.61935 m^2
Inner hydraulic diameter	0.0336 m
Overall volume	0.02427 m^3
Annulus hydraulic diameter	0.0331

The increase in pumping power is 2.0 times and 5.6 times for the first and second fractal exchanger, respectively.

EXPERIMENTAL STUDY

The numerical results were supplemented with experimental results, as the $n = 1$ fractal tube was manufactured and tested. The fractal tube was extruded in four aluminium sections, which were then welded together to form the fractal tube. The tube thickness was 3 mm to allow for welding and to prevent any leaks. The physical dimensions are shown in Table 2.

The experimental setup is shown in Figure 8. The hot water was pumped from the hot water tank to the inner tube of the heat exchanger. The cold water was pumped from the cold water

tank and flowed in the annulus in a counterflow direction. Both the hot and cold water's temperature could be set. Before the water returned to the tanks, they flowed through flow meters. The whole heat exchanger was insulated to ensure that no heat transfer to the environment took place.

The temperature was measured with K-type thermocouples. The thermocouples were connected to a calibrated Fluke meter. The temperatures that were measured were the hot and cold water inlet and outlet temperatures.

The flow was measured with a semi-rotary circular piston (also known as an oscillating piston) meter. The flow meter continually counted the amount of fluid flowing through it and displayed the amount as cubic meters.

The inlet and outlet hot and cold water temperatures were taken at different flow rates. For each set of flow rates, several measurements were taken, and the energy balance was calculated. An acceptable error for the heat transfer balance was assumed to be less than 5%. The error was calculated as the difference between the average and the inner heat transfer. The average heat transfer was calculated as the arithmetic mean of the inner and annulus heat transfer values.

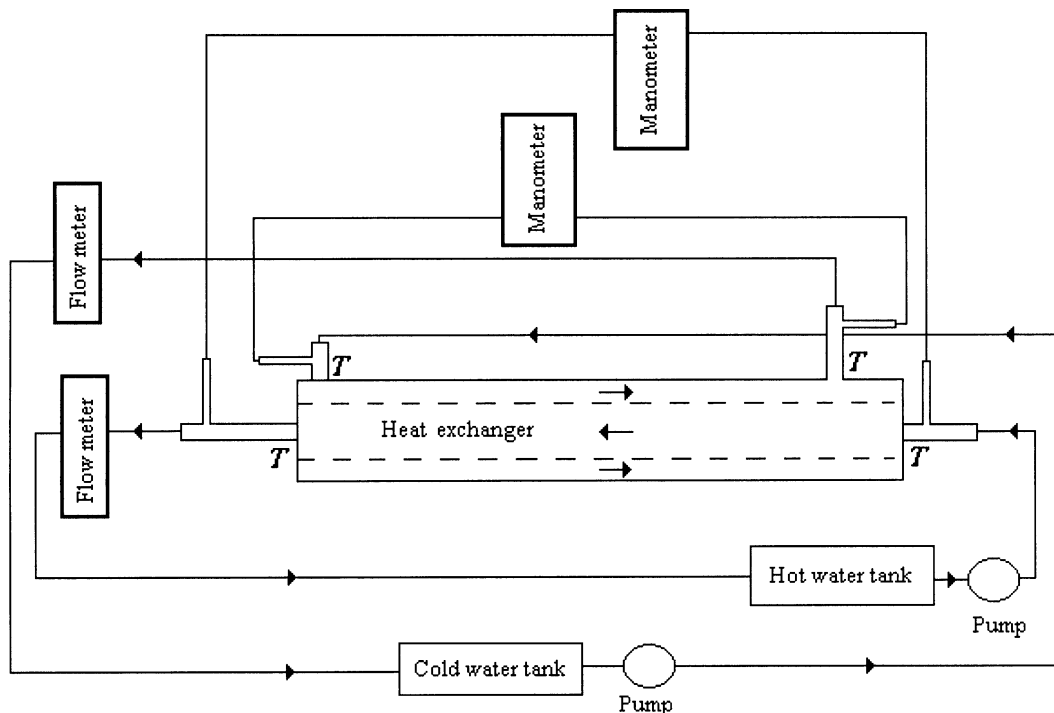


Figure 8 Experimental setup.

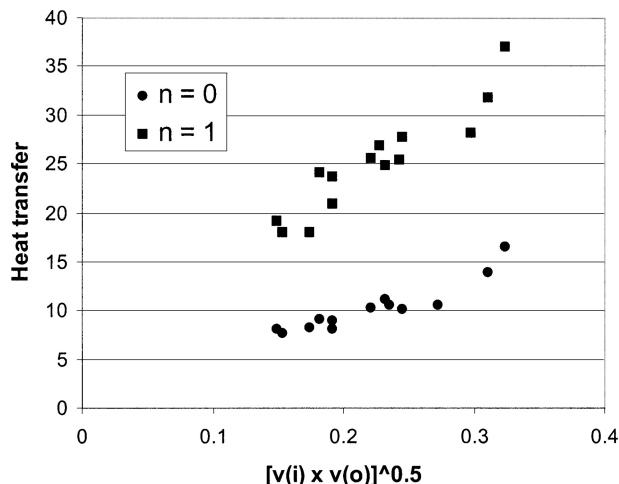


Figure 9 Experimental heat transfer of the fractal heat exchangers.

The fractal heat exchanger's performance was compared to an exchanger with no fractal iteration. This exchanger was a simple square inside-tube exchanger with a round outer tube (similar to Figure 2a). To compare the exchangers, it was decided that the inner cross-sectional area should be the same as the experimental exchanger. Thus, the inner square side's lengths were equal to 0.0336 m. The outer square side lengths were the inner length plus twice the thickness of 3 mm and had a value of 0.0396 m. The length and inner diameter of the outer tube remains the same. Table 3 displays the other dimensions.

The average increase in heat transfer per volume ratio was found to be 2.5 times. This is higher than the anticipated double increase. (Figure 9 shows the results.) This means that other factors, such as the heat transfer coefficient, were also a function of the fractal iteration.

CONCLUSION

An analytical heat transfer analysis was done to a quadratic Koch island fractal heat exchanger, and it was found that heat transfer increases with every application of the fractal, at least doubling at every fractal iteration. The prediction was validated numerically. The results show an increase of 2.1 ($n = 1$) and 3.9 ($n = 2$) times over the benchmark exchanger. The overall size of the exchanger increased by 50% ($n = 1$) and 63% ($n = 2$) over the benchmark exchanger.

One of the numerical prediction cases was validated with experimental results. The experimental study produced an increase of almost 2.5 times over the benchmark exchanger, which agrees well with the numerical prediction of 2.1 times. Because the increase was higher than expected, there were other factors such as the heat transfer coefficients that were also contributing to the heat transfer increase.

NOMENCLATURE

A	area, m ²
C	circumference, m
d	inner width or diameter of outer tube, m
d_h	hydraulic diameter, m
d_i	inner width of inner tube, m
d_o	outer width of inner tube, m
Δd	thickness of inner tube, m
D	dimension
f	scale factor
h	convective heat transfer coefficient, W/m ² K
H	height, m
k	thermal conductivity, W/mK
L	length, m
n	amount of iterations
N	amount of copies
Nu	Nusselt number
P	pumping power, W
p_w	perimeter evaluated at wall conditions, m
Pr	Prantl number
q	heat transfer, W
Re	Reynolds number
s	fractal segment length, m
T	temperature measuring points
ΔT	temperature difference, K, °C
U	overall heat transfer coefficient, W/m ² K
v	velocity, m/s
x_0	original length of one of the square's sides, m

Greek Symbols

ε	dissipation rate
μ	dynamic viscosity, Pa · s
κ	turbulent kinetic energy
ρ	density kg/m ³

Subscripts

i	inner
$LMTD$	log mean temperature difference
n	amount of iterations
o	annulus, outer

REFERENCES

- [1] Krenz, J. H., *Energy Conversion and Utilization*, 2nd ed., p. 2, Allyn and Beacon, Inc., Boston, 1984.
- [2] Griffin, J. M., and Steele, H. B., *Energy Economics and Policy*, p. 311, Academic Press, New York, 1980.

- [3] Samavati, H., Hajimiri, A., Shahani, A. R., Nasserbakht, G. N., and Lee, T. H., Fractal Capacitors, *IEEE Journal of Solid-State Circuits*, vol. 33, pp. 2035–2041, 1998.
- [4] Peitgen, H., Jürgens, H. and Saupe, D., *Fractals for the Classroom*, Part 1, 1st ed., pp. 229–239, Springer-Verlag, New York, 1993.
- [5] Nicolleau, F., and Mathieu, J., Eddy Break-up Model and Fractal Theory: Comparisons with Experiments, *Int. Journal of Mass and Heat Transfer*, vol. 37, pp. 2925–2933, 1994.
- [6] Farias, T. L., Carvalho, M. G., Köylü, Ü. Ö., and Faeth, G. M., Computational Evaluation of Approximate Rayleigh-Debye-Gans/Fractal-Aggregate Theory for the Absorption and Scattering Properties of Soot, *Journal of Heat Transfer*, vol. 117, pp. 152–159, 1995.
- [7] Tang, Z., and Hu, W., Fractal Features of Oscillatory Convection in the Half-Floating Zone, *Int. Journal of Mass and Heat Transfer*, vol. 38, pp. 3295–3303, 1995.
- [8] Ueki, Y., Tsuji, Y., and Nakamura, I., Fractal Analysis of a Circulating Flow Field with Two Different Velocity Laws, *European Journal of Mechanics-B/Fluids*, vol. 18, pp. 959–975, 1999.
- [9] Kacimov, A. R., and Obnosov, Y. V., Conduction through a Grooved Surface and Sierpinski Fractals, *Int. Journal of Mass and Heat Transfer*, vol. 43, pp. 623–628, 2000.
- [10] Majumdar, A., and Tien, C. L., Fractal Network Model for Contact Conductance, *Journal of Heat Transfer*, vol. 113, pp. 516–525, 1991.
- [11] Pitchumani, R., and Yao, S. C., Correlation of Thermal Conductivities of Unidirectional Fibrous Composites Using Local Fractal Techniques, *Journal of Heat Transfer*, vol. 113, pp. 788–796, 1991.
- [12] Chen, Y., and Cheng, P., Heat Transfer and Pressure Drop in Fractal Tree-Like Microchannel Nets, *International Journal of Heat and Mass Transfer*, vol. 45, pp. 2643–2648, 2002.
- [13] Holman, J. P., *Heat Transfer*, 3rd ed., pp. 2–34, 550–551, McGraw-Hill Book Company, London, 1992.
- [14] Shah, R. K., *A Short Course on Compact Heat Exchangers*, Unpublished course notes, pp. 1.4–1.5, 2000.



Josua P. Meyer obtained his B.Eng. (cum laude) in 1984, his M.Eng. (cum laude) in 1986, and his Ph.D. in 1988, all in Mechanical Engineering from the University of Pretoria. He is registered as a professional engineer and has completed his military service at the Faculty of Military Science, University of Stellenbosch, where he lectured aerodynamics for pilots in the South African Air Force. After his military service (1988–1989), he accepted a position as Associate Professor in the Department of Mechanical Engineering at the Potchefstroom University in 1990. He was Acting Head and Professor in Mechanical Engineering before accepting a position as professor in the Department of Mechanical and Manufacturing Engineering at the Rand Afrikaans University in 1994. He was the Chairman of Mechanical Engineering from 1999 until the end of June 2002, after which he was appointed as Professor and Head of the Department of Mechanical and Aeronautical Engineering of the University of Pretoria. He specializes in heat transfer, fluid mechanics, and thermodynamic aspects of heating, ventilation, and airconditioning. He is the author and co-author of more than 170 articles, conference papers and patents, and has received various prestigious awards for his research. He is also a fellow or member of various professional institutes and societies (i.e., South African Institute for Mechanical Engineers, South African Institute for Refrigeration and Air Conditioning, American Society for Mechanical Engineers, American Society for Air-Conditioning, Refrigeration and Air-Conditioning) and is regularly invited to be a keynote speaker at local and international conferences. He has also received various teaching awards as Lecturer of the Year (at the Potchefstroom University and Rand Afrikaans University). He is a rated researcher by the NRF and an Associate Editor for *Heat Transfer Engineering*.



Hilde van der Vyver is a lecturer at the Department of Mechanical Engineering at the Rand Afrikaans University, South Africa. She received her doctorate, from the same university in 2003 in the field of heat exchangers. Her main research interests are heat exchangers, computational fluid dynamics, and solar energy.

Copyright of Heat Transfer Engineering is the property of Taylor & Francis Ltd. The copyright in an individual article may be maintained by the author in certain cases. Content may not be copied or emailed to multiple sites or posted to a listserv without the copyright holder's express written permission. However, users may print, download, or email articles for individual use.

Copyright of Heat Transfer Engineering is the property of Taylor & Francis Ltd. The copyright in an individual article may be maintained by the author in certain cases. Content may not be copied or emailed to multiple sites or posted to a listserv without the copyright holder's express written permission. However, users may print, download, or email articles for individual use.